

Theory of Liquid Crystal Anchoring at a Porous Surface

David L. Cheung^{1,*}

¹*Department of Physics and Centre for Scientific Computing,
University of Warwick, Coventry, CV4 7AL, UK*

Using classical density functional theory (DFT) the effect of bringing a liquid crystal (LC) into contact with a porous substrate or matrix is investigated. The DFT used is a combination of the Onsager approximation to evaluate the excess free energy of the LC fluid and quenched annealed DFT to evaluate the interaction between the fluid and the porous substrate. When the fluid alignment far from the substrate is held perpendicular to its surface there is a thin layer of fluid aligned parallel to the substrate surface for low matrix densities. For higher matrix densities this director deformation propagates into the bulk of the fluid. Consideration of a system without confining walls suggests that for low matrix densities normal alignment is metastable compared to parallel alignment, while for higher matrix densities it is unstable.

I. INTRODUCTION

The interaction between liquid crystals (LC) and solid substrates of great interest, both scientific and technological¹. The presence of the surface both breaks the symmetry of the LC phases and often leads to alignment in a given direction. This tendency, often called anchoring, is vital to the use of LC in display applications and can be profoundly influenced by the structure of the surface.

Commonly surfaces may be rough or porous, e.g. SiO₂^{2,3}, which can lead to deviations from the behaviour expected from smooth surfaces⁴. A porous substrate or matrix may be regarded as a system of immobilised particles. Recent simulations of LC near rough walls^{5,6} using such a model have shown that properties such as the an-

choring coefficient and transition pressures of a confined LC are influenced by the roughness of the substrate. Due to the computational expense only a few surfaces at a given roughness were studied. It would thus be desirable to study a larger (ideally infinite) number of surfaces.

One route to this is through replica or quenched annealed density functional theory (QA-DFT)^{7,8,9,10}. In this the system comprises two components: the first, the quenched component, models the porous substrate, the second, the annealed component, models the fluid. The density distribution of the matrix, averaged over all matrix realisations, is determined through minimisation of a grand potential in the absence of the fluid. The density distribution of the fluid is then found by minimising a grand potential containing both matrix and fluid densities. This theory is fully outlined in the following section,

along with details of the systems studied. The results that ensue from applying it to LC anchoring at porous surfaces are outlined in Sec. III. Finally brief summary of this work and suggestions for future work are given in Sec. IV

II. THEORY AND MODEL

A. Density functional theory

In QA-DFT the grand potential is the sum of the grand potential of the matrix alone and the grand potential of

the fluid and matrix together, i.e. $\Omega[\rho_m(\mathbf{r}, \mathbf{u}), \rho_f(\mathbf{r}, \mathbf{u})] = \Omega_m[\rho_m(\mathbf{r}, \mathbf{u})] + \Omega_f[\rho_m(\mathbf{r}, \mathbf{u}), \rho_f(\mathbf{r}, \mathbf{u})]$ ⁷. Here we are interested in uniaxial molecules characterised by a position \mathbf{r} and orientation \mathbf{u} . For an ideal matrix (i.e. with vanishing interactions between the matrix particles) $\Omega_m[\rho_m(\mathbf{r}, \mathbf{u})]$ is

$$\beta\Omega_m[\rho_m(\mathbf{r}, \mathbf{u})] = \int d\mathbf{r}d\mathbf{u} \rho_m(\mathbf{r}, \mathbf{u}) \{ \log \rho_m(\mathbf{r}, \mathbf{u}) - 1 + \beta V_m(\mathbf{r}, \mathbf{u}) - \beta\mu_m \} \quad (1)$$

where $V_m(\mathbf{r}, \mathbf{u})$ is the external potential acting on the matrix, μ_m is its chemical potential, and $\beta = 1/k_B T$. If the external potential $V_m(\mathbf{r}, \mathbf{u})$ is used to confined the matrix to a region of space then the matrix grand po-

tential may be minimised analytically to give $\rho_m(\mathbf{r}, \mathbf{u}) = \rho_m = \exp(\beta\mu_m)$ inside this region and 0 outside it.

The grand potential for the fluid component is

$$\begin{aligned} \beta\Omega_f[\rho_f(\mathbf{r}, \mathbf{u}), \rho_m(\mathbf{r}, \mathbf{u})] = & \int d\mathbf{r}d\mathbf{u} \rho_f(\mathbf{r}, \mathbf{u}) [\log \rho_f(\mathbf{r}, \mathbf{u}) - 1] + \beta \int d\mathbf{r}d\mathbf{u} [V(\mathbf{r}, \mathbf{u}) - \mu] \rho_f(\mathbf{r}, \mathbf{u}) \\ & + \beta F_{\text{ex}}[\rho_f(\mathbf{r}, \mathbf{u})] + \beta F_{\text{ex}}^{mf}[\rho_f(\mathbf{r}, \mathbf{u}), \rho_m(\mathbf{r}, \mathbf{u})] \end{aligned} \quad (2)$$

where $\rho_f(\mathbf{r}, \mathbf{u})$ is the density distribution of the fluid component, $V(\mathbf{r}, \mathbf{u})$ is the external potential acting upon it, and μ is the fluid chemical potential. $F_{\text{ex}}[\rho_f(\mathbf{r}, \mathbf{u})]$ and $F_{\text{ex}}^{mf}[\rho_f(\mathbf{r}, \mathbf{u}), \rho_m(\mathbf{r}, \mathbf{u})]$ are the excess free energies due to

interactions between the fluid molecules and fluid-matrix molecules respectively. From hereon in the subscript f denoting the fluid component will be omitted. The excess

FE is evaluated within the Onsager approximation¹¹

$$\beta F_{\text{ex}}[\rho(\mathbf{r}, \mathbf{u})] = -\frac{1}{2} \int d\mathbf{r}_1 d\mathbf{u}_1 d\mathbf{r}_2 d\mathbf{u}_2 f(\mathbf{r}_{12}, \mathbf{u}_1, \mathbf{u}_2) \rho(\mathbf{r}_1, \mathbf{u}_1) \rho(\mathbf{r}_2, \mathbf{u}_2) \quad (3)$$

where $f(\mathbf{r}_{12}, \mathbf{u}_1, \mathbf{u}_2)$ is the Mayer function. For convenience we assume that the interaction between the matrix and fluid particles is identical to the interactions between the fluid particles.

In this work we are only concerned with systems that vary in the z direction only; the surfaces are assumed to be homogeneous in the x and y directions. The method

for finding the equilibrium density is the same as in previous work^{12,13}; the density and its logarithm are expanded in spherical harmonics

$$\rho(z, \mathbf{u}) = \sum_{\ell m} \rho_{\ell m}(z) Y_{\ell m}^*(\mathbf{u}) \quad (4a)$$

$$\log \rho(z, \mathbf{u}) = \sum_{\ell m} \tilde{\rho}_{\ell m}(z) Y_{\ell m}(\mathbf{u}) \quad (4b)$$

where $Y_{\ell m}(\mathbf{u})$ is a spherical harmonic. The Mayer function is expanded in rotational invariants. Inserting these into the grand potential (Eq. 2) and integrating over angles and the x and y axes gives

$$\begin{aligned} \beta \Omega_f[\rho(\mathbf{r}, \mathbf{u}), \rho_m(\mathbf{r}, \mathbf{u})] = & \int dz \sum_{\ell m} \rho_{\ell m}(z) \left\{ \tilde{\rho}_{\ell m}(z) + \beta V_{\ell m}(z) - \sqrt{4\pi} (1 + \beta \mu) \delta_{\ell 0} \right\} \\ & - \int dz_1 dz_2 \sum_{\ell_1 \ell_2 m} A_{\ell_1 \ell_2 m}(z_1 - z_2) \rho_{\ell_1 m}(z_1) \left(\rho_{\ell_2 m}(z_2) - \frac{1}{\sqrt{4\pi}} \rho_m(z_2) \delta_{\ell_2 0} \right) \end{aligned} \quad (5)$$

where $V_{\ell m}(z)$ are the spherical harmonics coefficients of the external potential and $A_{\ell_1 \ell_2 m}(z_1 - z_2)$ are the spherical harmonics coefficients of the excluded area¹². $\rho_m(z)$ is the matrix density, equal to ρ_m for $z_{\min} \leq z \leq z_{\max}$ and 0 otherwise. The equilibrium fluid density is then found by numerically minimising this with respect to $\tilde{\rho}_{\ell m}(z)$ using the conjugate gradients method¹⁴. When needed $\rho_{\ell m}(z)$ are found from Eqs. 4. Once the $\rho_{\ell m}(z)$ that minimises Ω_f has been found the fluid density profile is given by $\rho(z) = \int d\mathbf{u} \rho(z, \mathbf{u})$. The orientational ordering of the

fluid is described through the ordering tensor

$$Q_{\alpha\beta}(z) = \frac{3}{2} \int d\mathbf{u} \rho(z, \mathbf{u}) u_\alpha u_\beta - \frac{1}{2} \delta_{\alpha\beta}, \quad \alpha, \beta = x, y, z. \quad (6)$$

The order parameter is given by the largest eigenvalue of $Q_{\alpha\beta}(z)$ and the director by the eigenvector associated with it.

Both the fluid and the matrix particles are modelled as hard ellipsoids of revolution of elongation $e = a/b = 15$. The chemical potential is set to $\mu = 2.0k_B$ well inside the nematic phase. This class of model have been well studied as model liquid crystals¹⁵. Two different systems

were considered. In the first the fluid is confined between two hard walls at $z = 0$ and $z = L = 200b$, with the matrix confined in the region $0 \leq z \leq z_{\max} = 30b$. The wall at $z = L$ is used to provided (homeotropic or planar) alignment far from the matrix. In the second system the matrix is placed in the centre of a periodic system of width $200b$. The fluid density is then minimised from starting states parallel and normal to the matrix surface.

III. RESULTS

A. Confined Geometry

Shown in Fig. 1 are the density and order parameter profiles for the slab geometry with both planar and homeotropic alignment at the far wall. In all cases far from the matrix $\rho(z)$ is constant. For the lowest matrix density ($\rho_m = 0.05b^{-3}$) the fluid density with the matrix is non-zero, although far lower than in the fluid outside the matrix. At larger ρ_m the fluid density inside the matrix is zero. The variation in $\rho(z)$ near the matrix surface depends on ρ_m and the alignment far from the matrix. For planar alignment (Fig. 1a) and $\rho_m < 0.25b^{-3}$ $\rho(z)$ drops smoothly from the bulk value at $z \approx 45b$ (one molecular length from the matrix surface) to 0 just inside the matrix. For larger values of ρ_m a peak appears in $\rho(z)$ at $z \approx 37.5b$ (half a molecular length from the surface), corresponding to an absorbed layer of molecules. $\rho(z)$ then drops sharply to 0 about one molecular diameter outside the matrix. For these ρ_m the matrix becomes im-

penetrable to the fluid and starts to behave like a rough hard wall⁸. When the far wall gives rise to homeotropic alignment $\rho(z)$ has a slight peak at $z \approx 40b$ for all ρ_m that grows stronger for increasing ρ_m . For the highest values of ρ_m studied however, this peak is weaker than in the corresponding system with planar alignment.

Shown in Fig. 1c are order parameter profiles ($S(z)$) for the confined LC with a far planar wall. In common with the density profiles these are constant far from the matrix, while for all ρ_m $S(z) = 0$ inside the matrix. For $\rho_m = 0.05b^{-3}$ $S(z)$ drops smoothly to 0 while for a slightly higher ρ_m a sharp peak appears just inside the matrix surface. At higher ρ_m $S(z)$ also drops smoothly from its bulk value to 0, although this occurs outside the matrix and over a smaller range of z . $S(z)$ for the far homeotropic wall is shown in Fig. 1d. The behaviour of $S(z)$ near the matrix surface differs markedly for different ρ_m . For low ρ_m there are two peaks in $S(z)$ either side of the matrix surface, while deeper in the matrix $S(z)$ goes to zero. At larger ρ_m the order parameter drops to 0 at the matrix surface.

For the system with far homeotropic alignment the behaviour of $S(z)$ near the matrix surface is influenced by the behaviour of the director. Plotted in Fig. 2 is $\theta(z)$, the angle between the director and the z axis (the wall normal). For low ρ_m the director lies parallel to the z -axis ($\theta(z) = 0$) far from the matrix surface. Near the matrix surface however, it abruptly changes to lie in the xy plane ($\theta(z) = 90^\circ$). This preference for parallel align-

ment may be understood as the matrix consists of disordered ellipsoids, so the interface between it and the fluid is equivalent to an isotropic-nematic interface. Previous studies of this and similar models^{16,17} have shown that the director prefers to lie in the plane of the interface. For $\rho_m > 0.26$ the preference for planar anchoring at the matrix surface leads to continuous director variation through the cell from homeotropic at the far wall to planar at the matrix surface. By contrast for the far planar wall is constant $\theta(z) = 90^\circ$ for all ρ_m .

B. Open Geometry

Density and order parameters for the open system are shown in Fig. 3. As can be seen for both the homeotropic and planar anchoring $\rho(z)$ and $S(z)$ are similar to those for the confined system: far from the matrix these are constant while close to the surface of the matrix these drop to smaller values. Also, with the exception of the $\rho_m = 0.05b^{-3}$ system, $\rho(z)$ drops to 0 within the matrix.

The behaviour of the director is different in the open system. When the initial configuration for the minimisation has the director aligned parallel to the matrix surface the director remains in this state. For an initial normal alignment the final state also has normal alignment when $\rho_m \leq 0.25b^{-3}$, while for higher ρ_m the final state has parallel alignment. This suggests that the normal alignment is metastable with respect to parallel alignment. In order to confirm this we calculate the surface free energy γ , given by the excess (over bulk) grand potential per unit

area¹⁸

$$\beta\gamma = \frac{\beta\Omega[\rho(\mathbf{r}, \mathbf{u})] - \beta\Omega_b[\rho_b(\mathbf{u})]}{2A} \quad (7)$$

where $\Omega_b[\rho_b(1)]$ is the bulk grand potential. This is plotted in Fig. 4 for both initial parallel and normal alignments. As may be seen for $\rho_m \leq 0.25b^{-3}$ γ is lower for parallel alignment, indicating that normal alignment is metastable. For higher ρ_m normal alignment is unstable and γ is identical for both initial conditions.

IV. CONCLUSION

In this paper the effect of bringing a liquid crystalline fluid into contact with a porous substrate has been studied using QA-DFT. It was found that aligning the LC parallel to the substrate surface is favourable to normal alignment. For matrices of low density normal alignment is found to be metastable, while for higher ρ_m it is unstable. This preference for parallel alignment is in agreement with studies of the nematic-isotropic interface for the same model.

There are a number of possible extensions to this work. It would be of interest to compare the QA-DFT results to those of computer simulations. Also interesting phenomenon in the vicinity of the nematic-isotropic transition that may be examined or for LC mixtures and for different interactions between the fluid and matrix particles.

Acknowledgements

The author would like to thank Mike Allen and Matthias Schmidt for helpful advice. This work was

funded by UK EPSRC and computational resources were provided by the Centre for Scientific Computing, University of Warwick.

* Electronic address: david.cheung@warwick.ac.uk

¹ B. Jerome, Rep. Prog. Phys. **54**, 391 (1992).

² R. Barberi and G. Durand, Phys. Rev. A **41**, 2207 (1990).

³ J. Papanek and P. Martinot-Lagarde, J. Phys. (France) II **6**, 205 (1996).

⁴ T. J. Sluckin, Physica. A **213**, 105 (1995).

⁵ D. L. Cheung and F. Schmid, J. Chem. Phys. **122**, 074902 (2005).

⁶ D. L. Cheung and F. Schmid, Chem. Phys. Lett. **418**, 392 (2006).

⁷ M. Schmidt, Phys. Rev. E **66**, 041108 (2002).

⁸ M. Schmidt, Phys. Rev. E **68**, 021106 (2003).

⁹ H. Reich and M. Schmidt, J. Stat. Phys. **116**, 1683 (2004).

¹⁰ M. Schmidt, J. Phys. Condens. Matter **17**, S3481 (2005).

¹¹ L. Onsager, Ann. N. Y. Acad. Sci **51**, 627 (1949).

¹² D. Andrienko and M. P. Allen, Phys. Rev. E **65**, 021704 (2002).

¹³ D. L. Cheung and F. Schmid, J. Chem. Phys. **120**, 9185 (2004).

¹⁴ W. H. Press, B. P. Flannery, S. A. Teukolsky, and W. T. Vetterling, *Numerical Recipes in Fortran* (Cambridge University Press, 1992), 2nd ed.

¹⁵ M. P. Allen, G. T. Evans, D. Frenkel, and B. M. Mulder, Adv. Chem. Phys. **86**, 1 (1993).

¹⁶ D. L. Koch and O. G. Harden, Macromolecules **32**, 219 (1999).

¹⁷ M. P. Allen, J. Chem. Phys. **112**, 5447 (2000).

¹⁸ J. P. Hansen and I. R. McDonald, *Theory of Simple Liquids* (Academic Press, New York, 1990), 2nd ed.

Figure Captions

Fig. 1. (a) Density profiles ($\rho(z)$) for confined LC with far planar wall. Solid line $\rho_m = 0.05b^{-3}$, dotted line $\rho_m = 0.10b^{-3}$, dashed line $\rho_m = 0.25b^{-3}$, long dashed line $\rho_m = 0.30b^{-3}$, and dot-dashed line $\rho_m = 0.40b^{-3}$. (b) Density profiles for confined LC with far homeotropic wall. Symbols as in (a). (c) Order parameter profiles ($S(z)$) for confined LC with far planar wall. Symbols as in (a). (d) Order parameter profiles for confined LC with far homeotropic wall. Symbols as in (a).

Fig. 2. Director angle $\theta(z)$ for confined LC with far homeotropic wall. Solid line shows $\rho_m = 0.05b^{-3}$, dotted line shows $\rho_m = 0.25b^{-3}$, dashed line shows $\rho_m = 0.26b^{-3}$, long dashed line shows $\rho_m = 0.30b^{-3}$ and dot-dashed line shows $\rho_m = 0.40b^{-3}$.

Fig. 3. (a) Density profiles for open system with parallel alignment. Solid line $\rho_m = 0.05b^{-3}$, dotted line $\rho_m = 0.10b^{-3}$, dashed line $\rho_m = 0.25b^{-3}$, long dashed line $\rho_m = 0.30b^{-3}$, and dot-dashed line

$\rho_m = 0.40b^{-3}$. (b) Density profiles for open system with perpendicular alignment. (c) Order parameter profiles for open system with parallel alignment. Symbols as in (a). (d) Order parameter profiles for open system with perpendicular alignment. Symbols as in (a).

Fig. 4. Surface free energy ($\gamma = \Omega - \Omega_b$) per unit length for open systems with parallel (solid line) and normal (dashed line).

Fig. 1

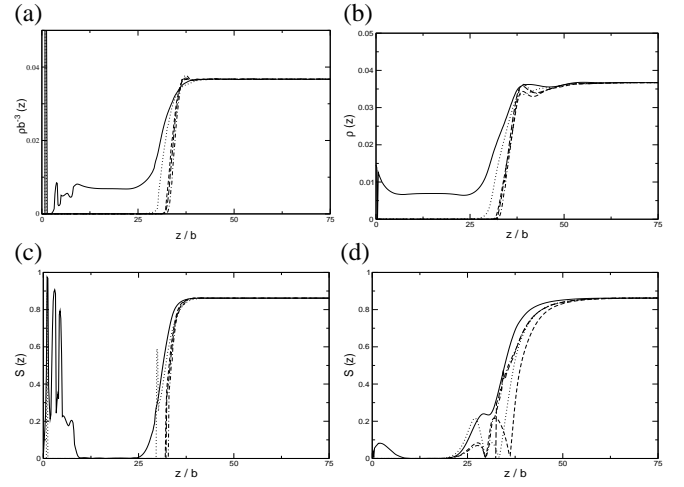


Fig. 2

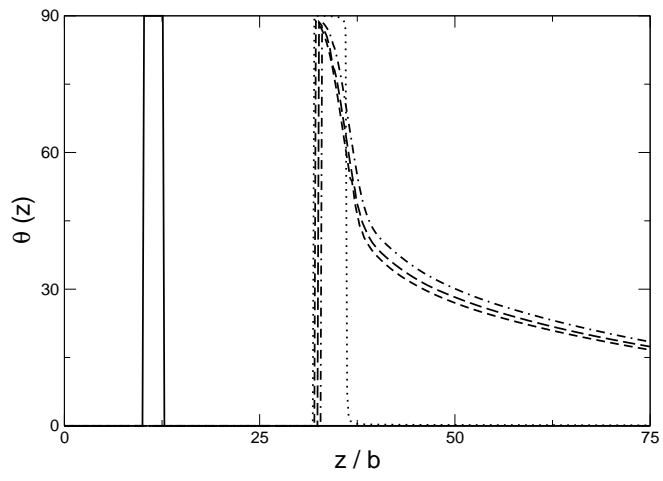


Fig. 3

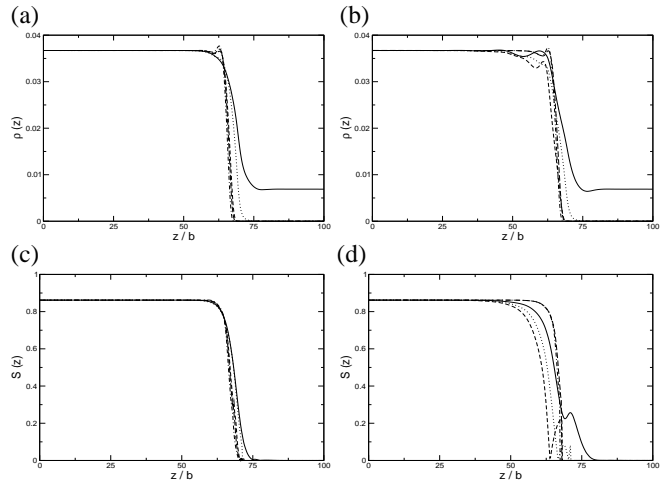


Fig. 4

